SUPPLEMENTAL MATERIAL FOR PAPER
"Observation of the resonance frequencies of a stable torus of fluid"

Claude Laroche,[1] Jean-Claude Bacri,[2] Martin Devaud,[2] Timothée Jamin,[3] and Eric Falcon[2]

[1] *Laroche Laboratory, Rue de la Madeleine, F-69 007 Lyon, France*
[2] *Université de Paris, Université Paris Diderot, MSC, UMR 7057 CNRS, F-75 013 Paris, France*
[3] *Université de Lyon, ENS de Lyon, CNRS, Lab. de Physique & UPMA, F-69342 Lyon, France*

In this supplemental material, we present experimental details (§1), movies (§2), pictures (§3), and additional measurements (§4) of the resonance frequencies of a fluid torus confined between two horizontal plates submitted to vertical sinusoidal oscillations. The derivation of the azimuthal eigenmodes of the torus is also presented in §5, as well as the flattening axisymmetric mode ($n = 1$) in §6, corresponding to Eqs. (1) and (2) of the paper, respectively. Notations as in the above-mentioned paper.

1. Experimental details

To accurately measure the onset of azimuthal oscillations of the torus, we process as follows. The shaker is driven sinusoidally at frequency f with a slowly increasing ramp in amplitude, A, the latter being controlled and measured by the voltage across the shaker over time (see Fig. 1). The photodiode measures the amplitude of the horizontal oscillations of the torus outer periphery over time. By comparing both amplitudes oscillating initially in phase at f (see left-hand side of Fig. 1), one can define accurately the onset of the instability when the fluid oscillations become slightly modulated in amplitude (see arrow in Fig. 1) as a precursor of the subharmonic behavior at $f/2$ of the fluid in response to the forcing at f (see right-hand side of Fig. 1).

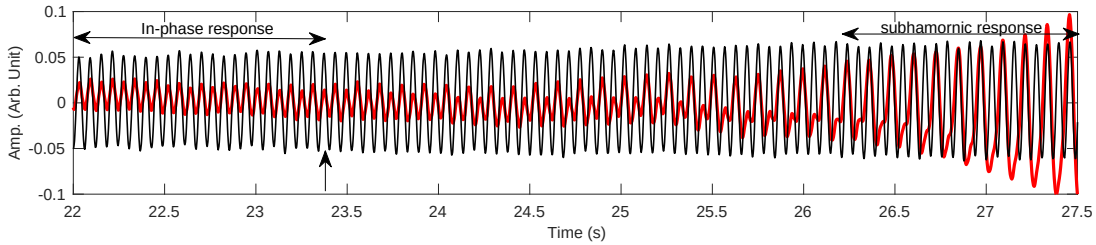

FIG. 1: Amplitude of horizontal oscillations of the fluid outer periphery (red-light grey curve) as a function of time in response to the vertical oscillations of the shaker (black curve). The arrow denotes the onset of the Faraday instability. In the right-hand side, the fluid oscillations are at half the forcing frequency. Mode 9. $f = 16.4$ Hz. $V = 1.5$ mL. $h = 1.5$ mm.

2. Movies

Top view of the azimuthal pattern at the outer periphery of a mercury torus. f: forcing frequency. n: number of lobes. 25 fps camera sampling. Note that the bright line corresponds to the specular reflection of the lighting, thus at a location just above the fluid outer periphery.

- mode7.mp4: Azimuthal mode $n = 7$ of a torus ($f = 10.9$ Hz),
- mode12.mp4: Azimuthal mode $n = 12$ of a torus ($f = 21.3$ Hz),
- mode16.mp4: Azimuthal mode $n = 16$ of a torus ($f = 32.2$ Hz),
- mode20.mp4: Azimuthal mode $n = 20$ of a torus ($f = 44$ Hz),
- a13.mp4: Poloidal deformations leading to axisymmetric mode of a puddle before the occurrence of the azimuthal mode $n = 8$. Constant forcing amplitude. $f = 11.6$ Hz. Similar observations occur for a torus.

3. Pictures

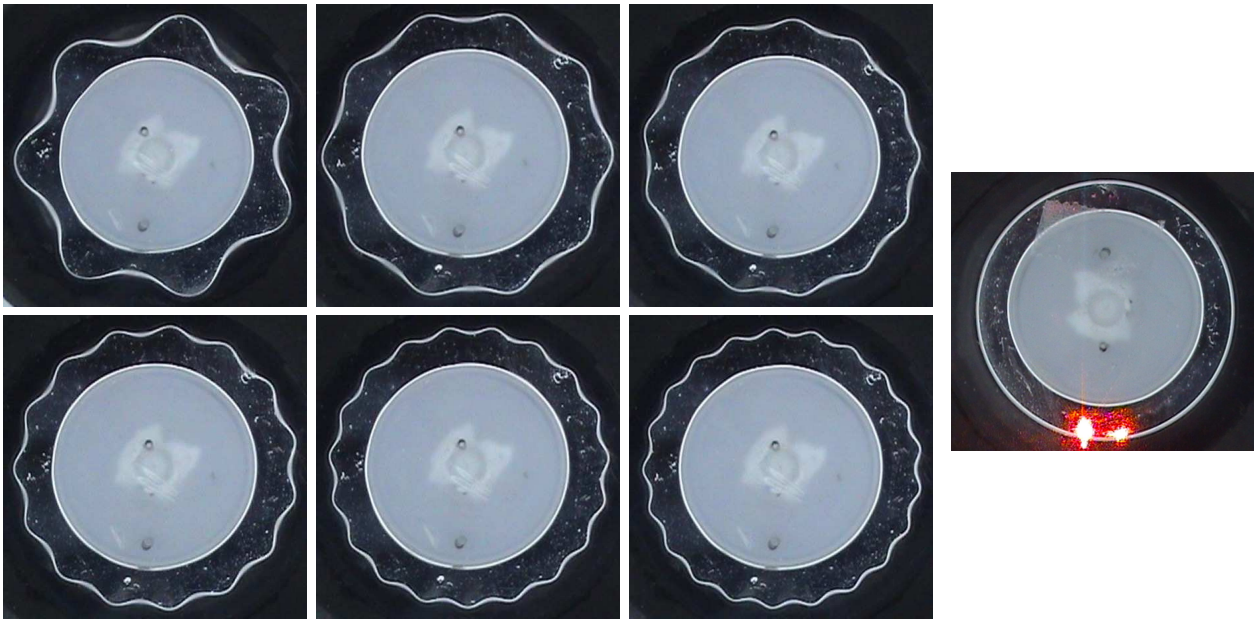

FIG. 2: Top view of the azimuthal pattern displayed around a torus of mercury for different increasing forcing frequencies f. The corresponding number n of lobes, oscillating at $f/2$ is $n = 7$, 10, 13, 15, 19 and 21, respectively (from left to right, top to bottom). Grey areas correspond to the central solid cylinder. Middle-right hand side: Static torus - no forcing ($f = 0$ Hz). Red laser spot is visible. Torus diameter at rest ≈ 42 mm. $V = 1.5$ mL. $h = 1.5$ mm.

4. Additional measurements of the resonance frequencies of a fluid torus

We reiterate experiments presented in the paper to measure the resonance frequency f_n of a fluid torus or of a puddle with different experimental parameters (puddle or torus radius R, height h between plates, shape and coating of the bottom plate). Figure 3 sums up the results. As shown in the main paper, f_n does not depend on the fluid geometry (see Fig. 3a - same in Lin-Lin as Fig. 5 of the main paper). Figure 3b shows experimental results when the bottom plate, slightly conical (angle of 1.4° with the horizontal [1]), is changed by a flat plate. No significant effect is observed. For a puddle, it is more difficult to reach its high resonance frequencies with a flat plate since it tends to drift from the center of the cell. Figure 3c shows results of experiments performed with or without hydrophobic coating of the bottom plate and for different h. Since the fluid volume is fixed, different h correspond also to different fluid radii R that we inferred from camera snapshots taken with no vibration. No significative effect of the hydrophobic coating appears here underlying that the natural unwetting of mercury is enough to obtain reproducible experiments. Note that, when working with a wetting fluid (e.g. water), it is generally crucial to minimize the pinning force of the drop at the contact line, with a hydrophobic coating of the substrate, to reach enough reproducible experiments [2, 3]. Finally, Fig. 3d reports, for a fixed fluid volume, the effect of the distance h between the top and bottom plates that are now fixed together, and thus oscillate in phase. Here again, no effect of h is noteworthy, and the prediction of Eq. (1) of the paper is well valid, for our tested h range.

5. Derivation of the azimuthal eigenmodes of a fluid torus

Let us consider a cylindrical torus of an unwetting fluid (such as mercury) with (at rest) radii R_i and R, and height h. The equilibrium pressure inside the fluid is homogeneous and equal to $P_0 = P_{\rm atm} + \gamma/R$. Let us use cylindrical coordinates and consider a fluid element, henceforth denoted $\vec{r}$, located at rest at point $\vec{r} = r\vec{e}_r + z\vec{e}_z$ ($r \in [R_i, R]$ and $z \in [0, h]$). In the framework of the Lagrange picture, this fluid element $\vec{r}$ is displaced in the course of the motion toward the point $\vec{s}(\vec{r}, t) = \vec{r} + \vec{\eta}(\vec{r}, t)$. Similarly, $P(\vec{r}, t)$ denoting the total pressure exerted upon element $\vec{r}$ at time t, the extrapressure field $p(\vec{r}, t)$ is defined by $P(\vec{r}, t) = P_0 + p(\vec{r}, t)$. Regarding mercury as an inviscid fluid, the motion

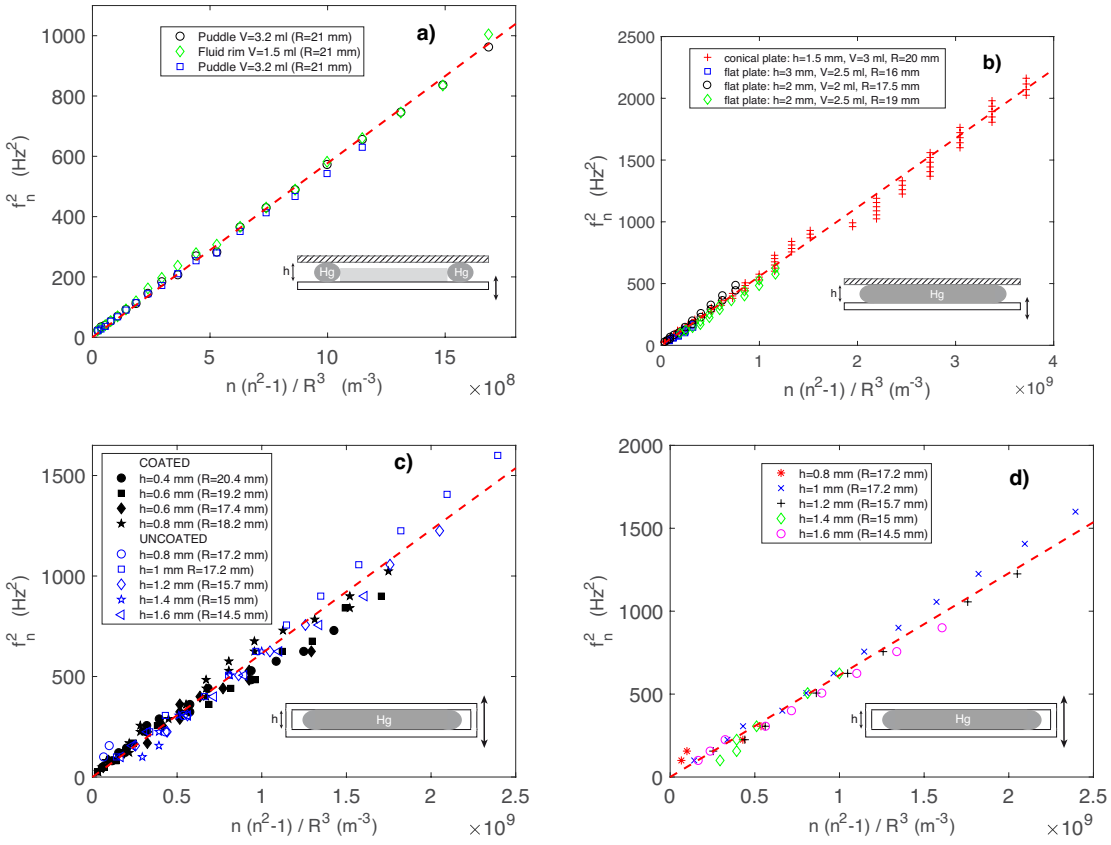

FIG. 3: Resonance frequency f_n of the mode n as a function of $n(n^2-1)/R^3$ for different experimental parameters. Dashed line corresponds to the prediction of Eq. (1) of the paper. (a) Fluid torus ($\Diamond$) or puddle ($\circ$, $\Box$). $h = 1.5$ mm. (b) Effect of the bottom plate shape: slightly conical plate ($+$), and flat plate (other symbols) for different h and V (corresponding to different fluid radii R). (c) With (full symbols) or without (open symbols) superhydrophobic coating of the bottom vibrating plate for different h (corresponding to different R) at fixed V. (d) Effect of distance h between the top and bottom plates. $V = 2$ mL. (a-b) top plate is fixed, and bottom plate is vibrating. (c-d) top and bottom plates are fixed together and oscillating in phase.

equation reads

$$\rho \frac{\partial^2 \vec{\eta}}{\partial t^2} = -\overrightarrow{grad}\, p \ . \tag{1}$$

Moreover, considering mercury as incompressible, we are left with $\Delta p = 0$. Allowing for the cylindrical symmetry of the problem (and for its assumed invariance along the z-direction), we can look for a solution of the latter equation of the form $p(r,\theta) = f(r)g(\theta)$, that is

$$\frac{1}{f(r)}\left(r^2\frac{d^2 f}{dr^2} + r\frac{df}{dr}\right) + \frac{1}{g(\theta)}\frac{d^2 g}{d\theta^2} = 0 \ . \tag{2}$$

Since function $g(\theta)$ is necessarily 2π-periodic, we should have $\frac{1}{g}\frac{d^2 g}{d\theta^2} = -n^2$, with n integer, involving $g(\theta) = \cos(n\theta + \psi)$, and consequently $r^2\frac{d^2 f}{dr^2} + r\frac{df}{dr} - n^2 f = 0$, and thus $f(r) = A_n r^n + A_{-n} r^{-n}$. Observe that a couple of solutions is associated to each value of integer n (corresponding to, say, $g_n(\theta) = \cos(n\theta)$ or $\sin(n\theta)$). It turns out that, in the linear approximation, each solution describes an eigenmode of azimuthal oscillation of the mercury torus. Let us focus on a given such mode, namely a given value of integer n with $g_n(\theta) = \cos(n\theta)$ and angular frequency ω_n. Using Eq. (1), we get

$$\vec{\eta}_n(r,\theta,t) = \frac{n\cos(\omega_n t)}{\rho\omega_n^2}\left[\left(A_n r^{n-1} - A_{-n} r^{-n-1}\right)\cos(n\theta)\vec{e}_r - \left(A_n r^{n-1} + A_{n-1} r^{-n-1}\right)\sin(n\theta)\vec{e}_\theta\right] \ . \tag{3}$$

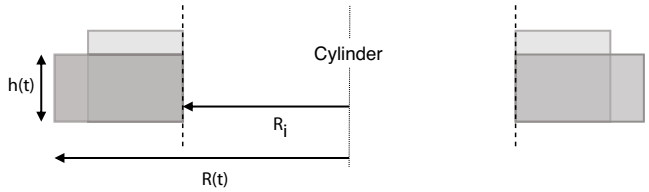

FIG. 4: Schematic lateral view of the flattening mode ($n = 1$) of a torus of rectangular section at two phases of its vibration.

Let us now consider the boundary conditions of our problem. For $r = R_i$, the radial component η_{nr} is necessarily zero, so that we have $A_{-n} = A_n R_i^{2n}$ and consequently

$$\eta_{nr}(r,\theta,t) = \frac{n\cos(\omega_n t)}{\rho\omega_n^2} A_n r^n \left[1 - \left(\frac{R_i}{r}\right)^{2n}\right] \cos(n\theta) \ . \tag{4}$$

For $r = R$ we have, due to the capillary Laplace law, $p(R) = P(R) - P_0 = P(R) - (P_{\rm atm} + \gamma/\rho) = \gamma/\mathcal{R} - \gamma/R$, where $\mathcal{R}$ is the radius of curvature of the free mercury surface. Now a careful calculation of $\mathcal{R}$ yields $\mathcal{R}^{-1} = R^{-1} - R^{-2}\left(\eta_r + \partial^2\eta_r/\partial\theta^2|_{r=R}\right)$, so that, for $n > 1$, we are left with

$$\omega_n^2 = \frac{\gamma}{\rho R^3} n(n^2-1)\frac{1 - \left(\frac{R_i}{R}\right)^{2n}}{1 + \left(\frac{R_i}{R}\right)^{2n}} \ , \tag{5}$$

that corresponds to the azimuthal eigenmodes of the torus given in Eq. (1) of the main paper. As expected, Eq. (5) with $R_i = 0$ reduces to the Rayleigh prediction valid for a puddle [4, 5]. Finally, it is noteworthy that the azimuthal oscillations of our mercury torus can be regarded as capillary waves at the surface of a cylindrical "ocean" with radii R_i and R, i.e. with a depth $R - R_i = 2a$. Integer n is just the number of wavelengths in the perimeter $2\pi R$. The associated wavenumber is $k = 2\pi/\lambda = n/R$. As a consequence, the dispersion relation reads from Eq. (5)

$$\omega^2(k) = \frac{\gamma}{\rho R^3} kR(k^2R^2-1)\frac{1 - \left(1 - \frac{2ak}{kR}\right)^{2kR}}{1 + \left(1 - \frac{2ak}{kR}\right)^{2kR}} \ . \tag{6}$$

It is interesting to examine the $kR \to \infty$ limit of the above formula. Indeed, we easily obtain $\omega^2(k) = (\gamma k^3/\rho)\tanh 2ak$, thus recovering the usual capillary waves dispersion relation for a finite liquid depth ($2a$).

6. Derivation of the flattening axisymmetric eigenmode ($n = 1$) of a fluid torus

For a puddle, this mode is usually called the breathing mode [6] or the radius pulsation mode [7]. Here we compute the frequency of the flattening axisymmetric mode of a torus of rectangular section by using conservation of energy when its shape is oscillating (see Fig. 4). The inner radius R_i is fixed, the outer radius $R(t)$ and the height $h(t)$ depend on time. Its volume $V = \pi h(t)\left[R(t)^2 - R_i^2\right]$ is conserved over time, which leads to $\frac{dh}{dt} = -\frac{2hR}{R^2-R_i^2}\frac{dR}{dt}$.

For a small variation of radius ΔR, the variation of potential energy $E_p = E_c + E_g$ with E_c the capillary energy and E_g the gravitational energy reads $\Delta E_p = \Delta R\frac{\partial E_p}{\partial R} + \frac{(\Delta R)^2}{2}\frac{\partial^2 E_p}{\partial R^2} + o[(\Delta R)^2]$. At equilibrium, $\partial E_p/\partial R = 0$. For $h \ll R - R_i$, effects of gravitational energy are negligible and the variation of capillary energy is mainly due to the variation of the top and bottom surfaces of the torus: $\frac{\partial^2 E_c}{\partial R^2} = 4\pi(\gamma_{solid/liquid} - \gamma_{solid/gas})$. As the contact angle between mercury and plates is close to 180°, we have $\gamma_{solid/liquid} - \gamma_{solid/gas} = \gamma$ and

$$\Delta E_p = \frac{1}{2}\frac{\partial^2 E_c}{\partial R^2}(\Delta R)^2 = 2\pi\gamma(\Delta R)^2. \tag{7}$$

If we suppose that radial velocity v_r only depends on r and vertical velocity v_z only depends on z, the boundary conditions and the condition of incompressibility yield to $v_r = R\frac{dR}{dt}(r - \frac{R_i^2}{r})/(R^2 - R_i^2)$. For $h \ll R - R_i$, the kinetic energy is dominated by radial motion:

$$E_k = \iiint \frac{\rho v_r^2}{2} dV = \frac{\pi \rho h R^2}{R^2 - R_i^2} \left(\frac{d\Delta R}{dt} \right)^2 \left(\frac{R^2 - 3R_i^2}{4} + \frac{R_i^4}{R^2 - R_i^2} \ln \frac{R}{R_i} \right) \tag{8}$$

By keeping the term in dR/dt of the lowest order (small fluctuations), conservation of energy $d(E_p + E_k)/dt = 0$ thus reads

$$\frac{d^2 \Delta R}{dt^2} + \omega_1^2 \Delta R = 0, \quad \text{with} \;\; \omega_1^2 = \frac{\gamma}{\rho h R^2} \cdot \frac{2(R^2 - R_i^2)}{\left(\frac{R^2 - 3R_i^2}{4} + \frac{R_i^4}{R^2 - R_i^2} \ln \frac{R}{R_i} \right)} \tag{9}$$

[1] For the bottom conical plate, the depth between the two plates is 2.4 mm at the center, and 1.5 mm at the tore/puddle periphery ($R = 21$ mm).
[2] F. Celestini and R. Kofman, Phys. Rev. E **73**, 041602 (2006).
[3] C.-T. Chang, J. B. Bostwick, P. H. Steen, and S. Daniel, Phys. Rev. E **88**, 023015 (2013).
[4] L. Rayleigh, Proc. R. Soc. London **29**, 71 (1879).
[5] H. Lamb, *Hydrodynamics* (Dover, New York, 1932), 6th ed.
[6] X. Ma and J. C. Burton, J. Fluid Mech. **846**, 263 (2018).
[7] X. Noblin, A. Buguin, and F. Brochard-Wyart, Phys. Rev. Lett. **94**, 166102 (2005).